บทความวิจัย

การตรวจวัดเชื้อแบคทีเรียก่อโรคแบบรวดเร็วโดยใช้อนุภาคนาโนเหล็กออกไซด์ซุปเปอร์พาราแมกเนติกด้วยแมกนีโตอิมพีแดนซ์เซ็นเซอร์ความไวสูง: การศึกษาเบื้องต้น

องอาจ เทียบเกาะ[1,*] กัลย์ชิญาภัท อริยะเชาว์กุล[2] มะลิวรรณ อมตธงไชย[3] และปุริม จารุจำรัส[3]

[1]ภาควิชาฟิสิกส์ คณะวิทยาศาสตร์ มหาวิทยาลัยอุบลราชธานี

[2]ภาควิชาวิทยาศาสตร์ชีวภาพ คณะวิทยาศาสตร์ มหาวิทยาลัยอุบลราชธานี

[3]ภาควิชาเคมี คณะวิทยาศาสตร์ มหาวิทยาลัยอุบลราชธานี

[*]Email: ongard.t@ubu.ac.th

รับบทความ: 13 เมษายน 2565 แก้ไขบทความ: 8 มิถุนายน 2565 ยอมรับตีพิมพ์: 13 มิถุนายน 2565

บทคัดย่อ

ความก้าวหน้าล่าสุดของการตรวจวัดสนามแม่เหล็กขนาดเล็กมากในระดับพิโคเทสลาภายใต้อุณหภูมิห้องโดยไม่มีการกำบังสนามแม่เหล็กภายนอกแสดงให้เห็นถึงศักยภาพในการนำวิธีดังกล่าวมาประยุกต์ใช้กับการทำเครื่องหมาย การติดฉลาก และการตรวจวัดทางแม่เหล็กของเป้าหมายเอกลักษณ์ทางชีวภาพ เช่น ไวรัส ยีนส์ โปรตีน และแบคทีเรีย ในบทความนี้ผู้วิจัยนำเสนอการตรวจวัดสนามแม่เหล็กของอนุภาคนาโนเหล็กออกไซด์ซุปเปอร์พาราแมกเนติกในอาหารเลี้ยงเชื้อแบบเหลว (Trypticase Soy Broth, TSB) และอนุภาคนาโนเหล็กออกไซด์ซุปเปอร์พาราแมกเนติกที่จับกับแบคทีเรียอีโคไล (*E. coli*) ในอาหารเหลว ซึ่งสนามแม่เหล็กของอนุภาคนาโนเหล็กออกไซด์ดังกล่าวที่จับกับแบคทีเรียอีโคไลถูกตรวจวัดได้ด้วยแมกนีโตอิมพีแดนซ์เซ็นเซอร์ความไวสูง ค่าแรงดันไฟฟ้าที่วัดได้จากแมกนีโตอิมพีแดนซ์เซ็นเซอร์ของตัวอย่างที่มีแบคทีเรียอีโคไลมีค่าต่ำกว่าค่าแรงดันไฟฟ้าที่วัดได้จากตัวอย่างควบคุมอย่างมีนัยสำคัญ วิธีการทำให้ตัวอย่างเป็นเนื้อเดียวกันก่อนการวัดและการนำสนามแม่เหล็กภายนอกขนาดประมาณ 0.2 มิลลิเทสลาไปยังตัวอย่างทำให้เกิดการปรับแต่งสัญญาณที่วัดได้เด่นชัดขึ้น และได้มีการศึกษาเบื้องต้นของการตรวจวัดอนุภาคนาโนเหล็กนาโนเหล็กออกไซด์ซุปเปอร์พาราแมกเนติกที่จับกับเชื้ออีโคไลที่ปนเปื้อนในเครื่องดื่ม เทคนิคและการตรวจวัดอย่างง่ายสำหรับอนุภาคนาโนแม่เหล็กนี้สามารถนำไปสู่การพัฒนาต่อยอดเป็นไบโอเซนเซอร์ขนาดกะทัดรัดที่สามารถพกพาได้

คำสำคัญ: อนุภาคนาโนเหล็กออกไซด์ซุปเปอร์พาราแมกเนติก แมกนีโตอิมพีแดนซ์เซ็นเซอร์ สนามแม่เหล็กขนาดเล็กมาก

Research Article

Rapid detection of Pathogenic Bacteria with Superparamagnetic Iron-oxide Nanoparticles (SPIONs) using highly sensitive magneto-impedance sensor: A preliminary study

Ongard Thiabgoh[1,*], Kanchiyaphat Ariyachaokun[2], Maliwan Amatatongchai[3] and Purim Jarujamrus[3]

[1]Department of Physics, Faculty of Science, Ubon Ratchathani University

[2]Department of Biological Science, Faculty of Science, Ubon Ratchathani University

[3]Department of Chemistry, Faculty of Science, Ubon Ratchathani University

[*]Email: ongard.t@ubu.ac.th

Received <13 April 2022>; Revised <8 June 2022>; Accepted <13 June 2022>

Abstract

Recent progress in the detection of ultra-small magnetic fields down to nano-Tesla level at room temperature and without magnetic shielding has shown potential applications in magnetic marking, labeling, and detecting for target biological entities such as viruses, genes, proteins, and bacteria. Herein, we present the detection of stray magnetic fields of superparamagnetic iron-oxide nanoparticles (SPIONs) in liquid medium (Trypticase Soy broth, TSB) and SPIONs bound to test bacteria (*Escherichia coli*). The stray magnetic fields of SPIONs captured *E. coli*, and that of the control samples were measured using a highly sensitive magneto-impedance (MI) sensor. The output voltage of MI-sensor of SPIONs-captured *E. coli* sample was significantly lower than the control samples. Homogenizing samples prior detection and the introduction of the external static magnetic field, $H_{ext,}$ of ~ 0.2 mT to the samples showed remarkable enhancement of magnetic signals. The preliminary study of SPIONs captured*E. coli* in dairy beverages has been performed. This simple and versatile technique for detecting magnetic nanoparticles can be further developed for a portable magnetic biosensor.

Keywords: superparamagnetic iron-oxide nanoparticles (SPIONs), magneto-impedance (MI) sensor, ultra-small magnetic fields

1. Introduction

The rapid detection of magnetic nanoparticles or magnetically labeled bioanalytes has been extensively investigated due to wide ranges of biosensing and biomedical applications (Anik *et al.,* 2021; Wang *et al.*, 2017; Zhong *et al*., 2021). It has been established that a significant change in the particle's size in nanometer scales of magnetic materials such as magnetite (Fe_3O_4), cobalt ferrite ($CoFe_2O_4$) (Liu *et al*., 2020), two-dimensional ferromagnetic monolayers (Bonilla et al., 2018), etc. can alter dramatically the physical and magnetic properties of the nanostructured materials (Krishnan, 2017). In particular, the emergence of magnetic nanoparticles exhibits unique magnetic properties such as the single domain, and the absence of remnant magnetization and zero coercivity of the magnetization curve of superparamagnetic nanoparticles. Recently, SPIONs have been intensively explored because of their tremendous potential applications in magnetic imaging, hyperthermia treatment, targeted drug delivery, and magnetic biosensing (Handa, 2018). To date, SPIONs can be tailored into a few nanometers via the synthesis process and used in targeted molecules or micro-organism of interest. Therefore, the rapid detection of magnetic signals from the SPIONs is highly promising for biosensor technology and medical diagnostics.

Stray magnetic fields generated from the magnetic nanoparticles are very small and not be able to detect using typical magnetic sensors. Only high sensitive magnetometers including giant magnetoresistance (GMR) sensor, superconducting quantum interference devices (SQUID), and giant magneto-impedance sensor (GMI) are capable to detect the weak magnetic fields (Makarov *et al*., 2016). Among the mentioned magnetic sensors, SQUID magnetometer is the most sensitive compared with the others; however, operating under the cryogenic environment makes it not suitable for a practical application. Recently, a highly sensitive GMI-based sensor has been employed for detecting stray magnetic fields of magnetic nanoparticles and magnetic beads tagged to pathogenic microorganism (Yang *et al*., 2015; 2016). Devkota *et al*. reported the detection of Nanomag-D beads using an acid-treated amorphous ribbon (Devkota *et al*., 2013a; Devkota *et al*., 2013b). Later, Yang *et al*. (2016) employed a giant magneto-impedance sensor on the antibodies modified with gold surface which resulted to ultrasensitive detection of injected *E. coli*-Dyabead complexes into a microfluidic device (MFD) prepared by MEM technology. Despite of high-sensitivity detection of *E. coli*-Dyabead, the fabrication of open-surface MFD is sophisticated and expensive. Hence, an alternative technique is needed in order to detect the weak field intensity from the targeting biomolecules or captured micro-organism using a contactless device or a magnetic nanoparticle-based test kit and reasonable cost.

Recently, MI-sensor developed by Nagoya University researchers has been used for the real-time measurement of biomagnetic fields in living systems (Uchiyama *et al*., 2009). This improved- magneto impedance sensor dramatically showed the weak-field detection down to nano-Tesla at a working distance of ~ 1 mm without magnetic shield (Nakayama and Uchiyama, 2015). Thus, the utility of the contactless MI-sensors and magnetic test for detecting magnetic signals from target materials with magnetic beads or functionalized magnetic nanoparticles will be an alternative technology for the development of future biosensors.

In this study, we present a new alternative technique for detecting stray magnetic field from SPIONs-captured pathogenic bacteria in TSB and contaminated beverages. A highly sensitive MI-sensor was employed to detect small magnetic fields down to nanoTesla range generated from SPIONs and SPIONs-captured *E. coli.* Moreover, versatile techniques using the application of an external static magnetic field, and homogenizing samples by vortexing showed the remarkable enhancement of magnetic signals from the samples relative to the controls.

2. Materials and Methods

2.1 Synthesis of Superparamagnetic Iron-oxide Nanoparticles (SPIONs)

In this experiment, the bottom-up approaches were employed to synthesize the magnetite nanoparticles. Thermal co-precipitation technique was used to synthesize the superparamagnetic iron-oxide nanoparticles (SPIONs), as detailed in our previous work (Sroysee *et al*., 2016). The semi-translucent samples of SPIONs were prepared for successfully transmission of electron beam through it. The sample size and shape were investigated by transmission electron microscopy (TEM, Model JEM-1230; JEOL, Tokyo, Japan) and operated under vacuum at an accelerating voltage of 20 kV. The magnetic property was investigated using vibrating-sample magnetometer (VSM). The optical images were taken using an optical camera: an Olympus CX23 with magnification of 1,000x.

2.2 Bacteria Preparation

Escherichia coli (ATCC 25922, Gram-negative bacteria) was streaked into Trypticase Soy agar (TSA) to obtain isolated colonies. After incubation at 37°C overnight, four or five colonies with an inoculating loop were selected and were transferred to a tube of Trypticase Soy broth (TSB) and then incubated for 3–5 h to standardize the culture to 1.5×10^8 CFU/mL (corresponding to 0.5 McFarland standards). Afterward, the culture was prepared about 1.00 mL for each experiment.

2.3 MI-Sensor Calibration and Detection of *E. coli* with SPIONs

The measurement of small magnetic fields using a commercial MI-sensor developed by Aichi Micro Intelligent Corporation (Mohri et al., 2009) was performed and calibrated. The magnetic field was generated using the paired coils (N = 154 turns, radius of 0.20 m) in Helmholtz arrangement developed by PHYWE: Science Education. The coils were connected in series and set-up in the same direction as earth magnetic field. Then, small currents of 3, 5, 10, 15, and 20 μA were applied to the coils in order to generate static magnetic fields 2.08, 3.46, 6.92, 10.38, and 13.84 nT at the coil center, respectively.

The MI-sensor, which possess detecting range of magnetic change between -40 μT to +40 μT, was located at the center of the Helmholtz coils to probe the presence of a relatively uniform magnetic field. A constant voltage of 5.00 volts was supplied the MI-sensor throughout the experiment. It is worth mentioning that the developed MI-sensor is designed for the measurement of the change in a dc magnetic field with respect to the previously static field, and the corresponding field sensitivity is ~ 1 mV/nT. The standard noise of the MI-sensor is ~200 pT/$\sqrt{Hz}$. Further details and specification of the product can be found in the data sheet of the product given by Aichi Micro Intelligent Corporation (Steel, 2022). The output voltage was read through a digital multimeter (mV resolution). The experimental setup is shown in Figure 1 (a).

Firstly, the detection of weak magnetic fields generated from 5, 10, and 15 mg of SPION suspension of 1.0 mL in microcentrifuge tubes were measured at a working distance 5 mm in order to evaluate the capability of our concepts as shown in Figure 1 (b). The sample holder was controlled by a stepper motor controller and an Arduino UNO board current driver at far-off distance ~ 60.00 cm and constantly rotating toward the MI-sensor with 4.0 rpm. All samples and controls were measured at the same positions and rotating speed.

Secondly, three pairs of the sample and control were prepared for the systematic detection of SPIONs-captured *E. coli.* The prepared *E. coli* samples and only TSB were added into microcentrifuge tubes containing 5, 10, and 15 mg of SPIONs for 1.0 mL. The suspension mixtures were mixed with vortex for 10 sec. Then, the samples and controls were ready for the stray field measurement. In order to enhance the detection of the stray fields generated from the samples, sample homogenization prior detection by vortexing, and the application of an external static magnetic field, H_{ext}, of ~ 0.2 mT toward the samples were systematically performed (Moghanizadeh *et al*., 2021).

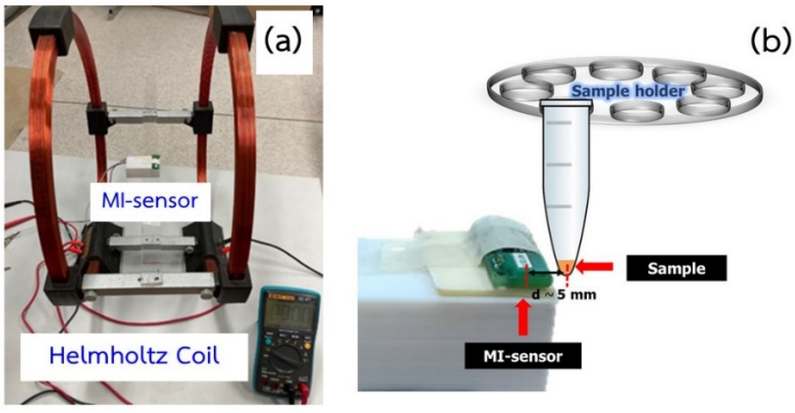

Figure 1. Experimental setup showing (a) magnetic field calibration using the Helmholtz arrangement and (b) schematic of the magnetic nanoparticles measurement.

Thirdly, the detection of *E. coli* contamination in dairy beverages purchased from our university canteen was carried out for iced coffee (S1), iced milk tea (S2), and chrysanthemum tea (S3), respectively. In the succeeding procedures, the amount of 10 mg SPIONs was selected for our further experiments because the experimental results drastically showed a large significant signal between the sample and the control. The sterilized iced coffee, iced milk tea, and chrysanthemum tea of 0.5 ml with SPIONs 10 mg were prepared for the bacterial contamination test. The amount of 0.5 ml of *E. coli* with concentration of 1.5 x 10^8 CFU/mL was added into the prepared beverages one-by-one. The controls of the sterilized iced coffee, iced milk tea, and chrysanthemum tea were added with TSB 0.5 mL, respectively. The sample preparation for the detection of *E. coli* with SPIONs is shown in Figure 2.

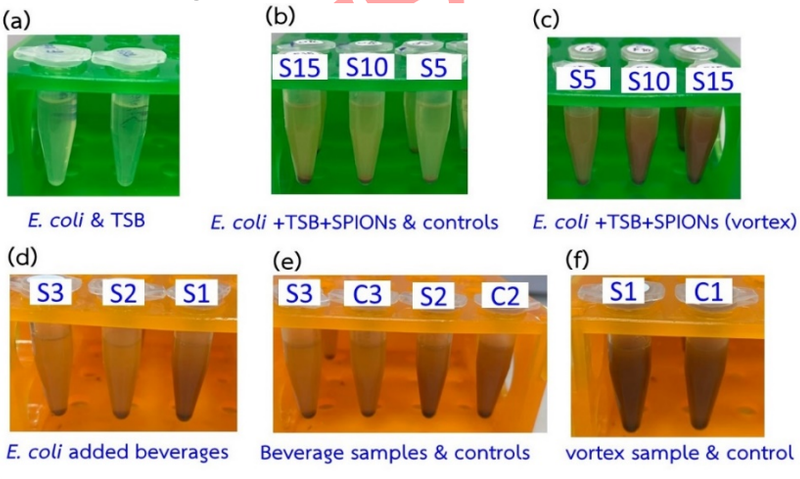

Figure 2. Experimental setup showing (a) *E. coli* suspension and only TSB, (b)-(c) *E. coli* and 5 mg (S5), 10 mg (S10), and 15 mg (S10) of SPIONs added for 1.0 ml., (d) *E. coli* spiked samples, (e) beverage samples & controls, and (d) beverage sample & control (vortex)

3. Results and Discussion

3.1 Material Characterization

When the magnetic material sizes reduce into nanoscales, the particle sizes of the materials play an essential role in physical and magnetic properties. Figure 3 (a) shows the particle size and morphology of magnetic nanoparticles synthesized by the thermal decomposition technique. The approximated size of the particles is ~ 10-15 nm and some of the nanoparticles is slightly smaller than the others. There is a slight difference in particle shape; however, their overall morphology remains similar. The size and morphology of the SPIONs play an essential role in magnetic properties. When the size of the magnetite is very small, the surface area to volume ratio becomes critical. As a results, this particle possesses only one single-domain

and exhibits superparamagnetic state. The critical diameters of the SPION are approximately few nanometers. In this state, the magnetic moments of the SPIOs will be aligned when an external magnetic field is applied (Krishnan, 2017). Furthermore, as the particle' size decreases in the ion state, the magnetic moments of SPIONs randomly flip direction under the influence of temperature because of the superparamagnetic state. The magnetization of the magnetic field curve at room temperature for the obtained ferrite nanoparticles is shown in Figure 3 (b). As can be seen in the Figure 3 (b), the absence of remnant magnetization and zero coercivity of the MH loop was observed from the samples. The maximum magnetization (M_s) of the Fe_3O_4 is ~ 9 emu/g which is in accordance with the previous works reported for small sizes of iron-oxide nanoparticles of ~15-20 nm.

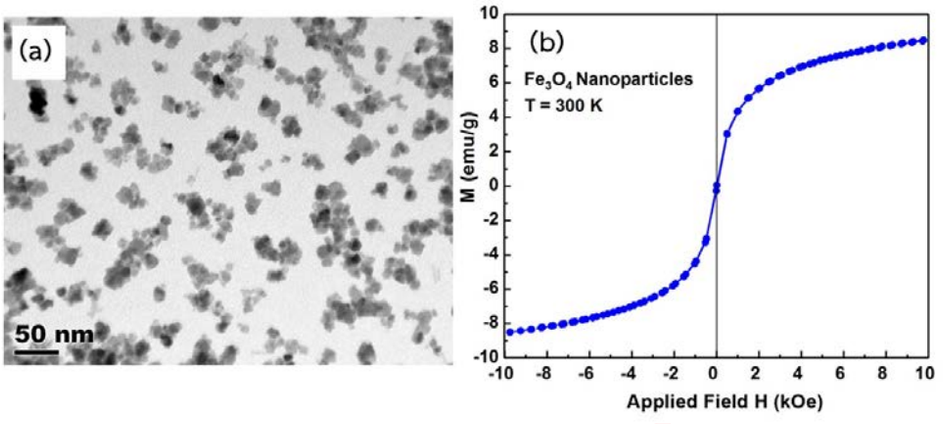

Figure 3. The sample size, shape and magnetic properties were investigated by (a) transmission electron microscopy (TEM), and (b) a vibrating-sample magnetometer (VSM), respectively.

3.2 Bacteria mixed with SPIONs

As mentioned previously, the ferrite nanoparticles are able to capture *E. coli. cells* owing to the electrostatic forces between positively charged particles of Fe_3O_4 in suspension and the negatively charged membrane of bacterial cells (Li *et al*., 2019; Quintana-Sánchez *et al.*, 2021). Figure 4(a) shows optical images of *E. coli* magnified by 1000x using an optical microscope. There is no SPION or their aggregation appears in the TSB and *E. coli* mixture. The bacteria mixed with 5, 10, and 15 mgs in TSBs (concentration ~ 1.5 x 10^8 CFU/mL) are shown in Figure 4 (b)-(d), respectively. As can be seen in the Figure 4 (b)-(d), some of SPION aggregation and *E. coli* are obviously observed under the microscope due to the typical sizes of the bacteria and SPION aggregation; however, a single SPION or finer SPIONs could not be observed through the light microscopy.

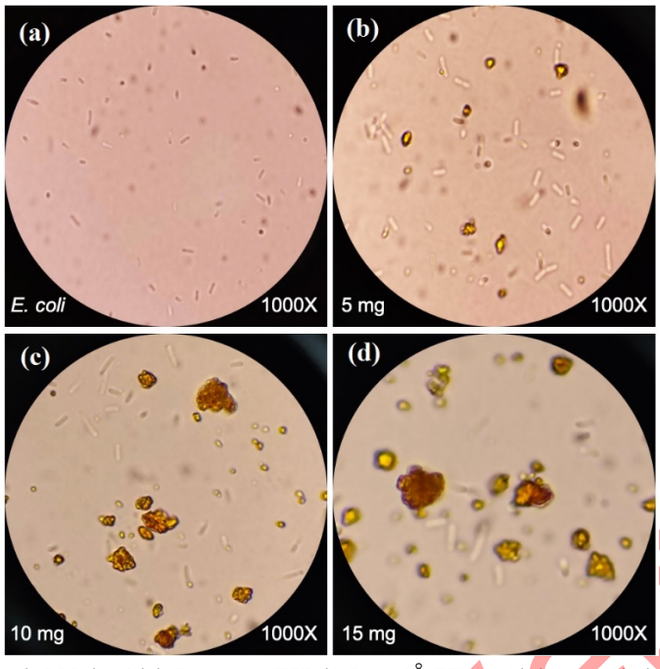

Figure 4. Optical images (1000x) of (a) *E. coli* in TSB (1.5 x 10^8 CFU/mL) (control), (b)-(d) *E. coli* mixed with various amount of SPIONs namely for 5, 10, and 15 mgs in TSB (1.5 x 10^8 CFU/mL), respectively.

3.3 Magneto-impedance Sensor Calibration

The measurement of weak magnetic fields at the center of the Helmholtz coils; 2.08, 3.46, 6.92, 10.38, and 13.84 nT was performed, respectively. The relationship between the expected magnetic fields and measured relative changes of the output potentials shows good linear characteristics. The field-detection sensitivity is approximately ~ 0.9865 mV/nT (Figure 5 (a)), which is slightly different from the given specification in the product data sheet (1.0 mV/nT). As expected, this experimental measurement of ultra-high sensitive magnetic fields was obviously reported for an amorphous wire MI sensor that are capable of sensing nT fields (Nakayama and Uchiyama, 2015). Figure 5 (b) shows the relative changes of the output potentials for the stray magnetic fields of SPIONs suspended in TSB 1.0 mL. The linear relationship between the amount of SPIONs and relative changes of the output potentials is observed. The corresponding output potentials are 3.83, 8.67, and 14.33 mV, for the solution with 5, 10 and 15 mgs, respectively. In our experiment, the stray magnetic fields of SPIONs in a powder form were investigated as well, and the detected fields are 5.83, 10.05, and 15.33 mV, respectively, which are slightly higher than the suspension one (not shown in the Figure). It is worth mentioning that there is no change in the output potentials of the MI-sensor when the *E. coli* and TSB without SPIONs was measured.

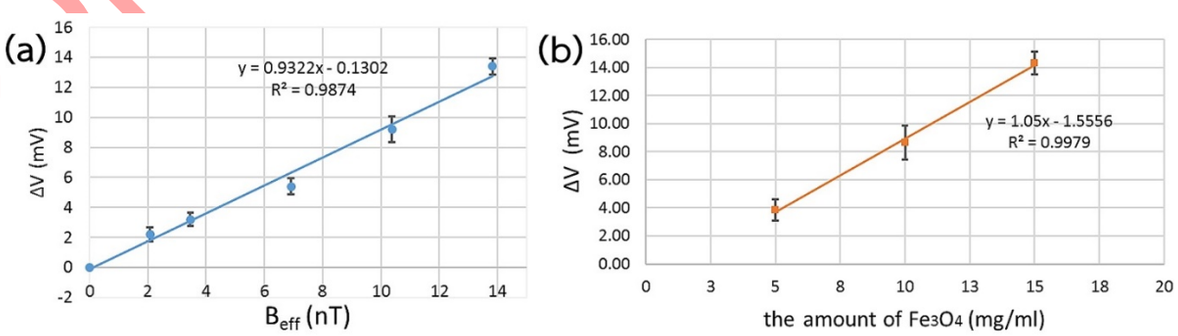

Figure 5. Relative magnetic field change for (a) each concentration of nanoparticles, the linear response for (b) the low concentration regime.

3.4 The detection of *E. coli* with SPIONs

To further investigate the stray field generated from magnetically captured bacteria by SPIONs, the comparison of the measured voltages subtracted from the blank control among various SPIONs controls was also performed. Figure 6 (a) shows the output voltages obtained from the MI-sensor from the samples and their controls at different SPION concentrations after the samples aggregated for 10 min. It is noticeable that there is a slight difference between the output voltage measured from the sample and the control for each concentration. As expected, the differences of the output voltages of the samples and controls (ΔV) are 0.67 mV (SPIONs, 5 mg), 0.67 mV (SPIONs, 10 mg), and 0.33 mV (SPIONs, 15 mg), respectively. In order to explore the larger changes of the output voltage, the method of sample homogenization prior the detection was prepared. As can be seen in Figure 6 (b), there is a significant difference between the output voltages and the controls. In particular, the change of the output voltage up to 2.67 mV was observed for the 10 mg concentration. The differences of the output voltages of the samples and controls (ΔV) are 1.00 mV (SPIONs, 5 mg), and 1.33 mV (SPIONs, 15 mg), respectively. In order to confirm the ability of the magnetically captured bacteria, the arrangement of an applied magnetic field of ~0.2 mT in downward direction was introduced toward the samples during the measurement (Moghanizadeh *et al*., 2021). Figure 6 (c) shows the enhancement of the output-voltage changes for all samples when the samples and their controls experienced an external magnetic field. The differences of the output voltages of the samples and controls (ΔV) are 1.67 mV (SPIONs, 5 mg), 2.00 mV (SPIONs, 10 mg), and 0.67 mV (SPIONs, 15 mg), respectively. Despite the enhancement of the measured output voltages with different SPIONs concentrations, the output-voltage is further enhanced by homogenizing the sample using the suspension technique.

It is established that stray magnetic fields generated from SPIONs, and SPIONs bounded *E. coli.* depends crucially on their shape anisotropy (Wu *et al*., 2015). If the SPIONs bounded *E. coli.* are not obviously aggregated down to the bottom caused by the gravitational field, the superimposed fields would be reduced compared with the control samples (Sandhu *et al*., 2018; Moghanizadeh *et al*., 2021). As expected, this process can be prevented by vortexing the mixtures before the measurement. Furthermore, the application of small static magnetic fields in downward direction try to push the SPIONs down to the bottom, which can decrease the horizontal stray magnetic fields toward the sensor. As a result, the overall output voltages decrease (see Figure 6(c)) (Mohri *et al.*, 2009; Steel, 2022).

In order to preliminary investigate the feasibility of the method in real practical application, the quasi-experiment setup of everyday contaminated beverages was simulated and explored. For proceeding experiment, only the amount of 10 mg SPIONs was selected to mix into iced coffee (S1), iced milk tea (S2), and chrysanthemum tea (S3) purchased from our university canteen. The MI-sensor was employed to measure the signal obtained from samples (namely control) and spiked samples. As mentioned in the experimental part, by employing 10 mg of SPIONs into the samples and controls (C1-C3), resulted to significant change in the outputs in comparison with the other concentrations as presented in the previous section. Figure 7 (a) shows the significant differences of the output voltages obtained from the iced coffee (ΔV~1.67 mV), iced milk tea (ΔV~2.67 mV), and chrysanthemum tea (ΔV~4.67 mV), from their controls. Furthermore, homogenization of the sample by vortexing of the mixtures for 10 seconds prior to the detection was also conducted. As with the case presented in the previous section, a significant difference of the output voltages of the samples and controls (ΔV) are detected, yielding 3.67, 4.33, and 4.67 mV, for S1, S2 and S3, respectively (see Figure 7 (b)). Similarly, there is also enhancement in the change of the output-voltage for all samples when the samples and their controls experienced the external magnetic field (H_{ext} ~0.2 mT) in downward direction (ΔV), yielding 1.33, 4.33, and 5.33 mV, for S1, S2 and S3, respectively (see Figure 7 (c)). As mentioned previously, the aggregation of SPIONs and SPIONs bounded *E. coli.* down to the bottom part plays an essential role in the differences of the output voltages of the samples and controls. As expected, similar to the results

of the TSB suspensions have also been observed, i.e., the sample homogenization prior detection and the application of external magnetic field enhance the magnetic signals (Handa, 2018; Moghanizadeh et al., 2021).

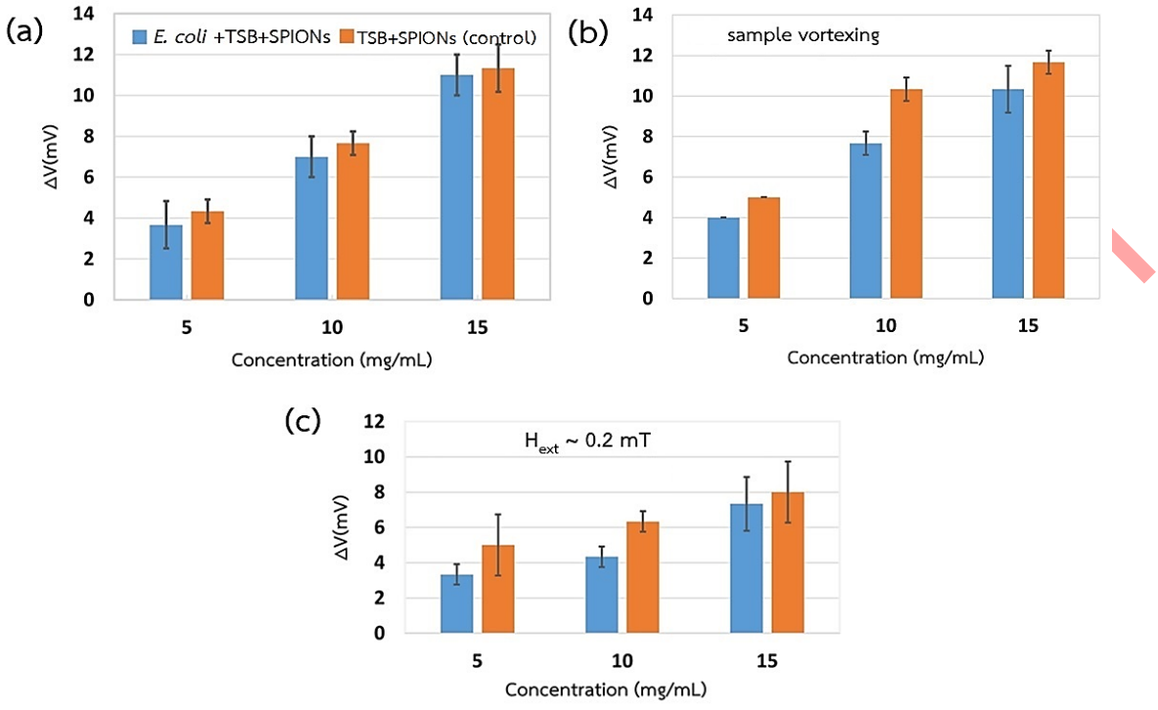

Figure 6. The output voltages of (a) the MI-sensor obtained from the samples and their controls at different SPIONs concentrations after aggregating the samples for 10 min, (b) after repeatedly homogenizing sample, and (c) when the magnetic field of ~0.2 mT was applied to the samples in downward direction.

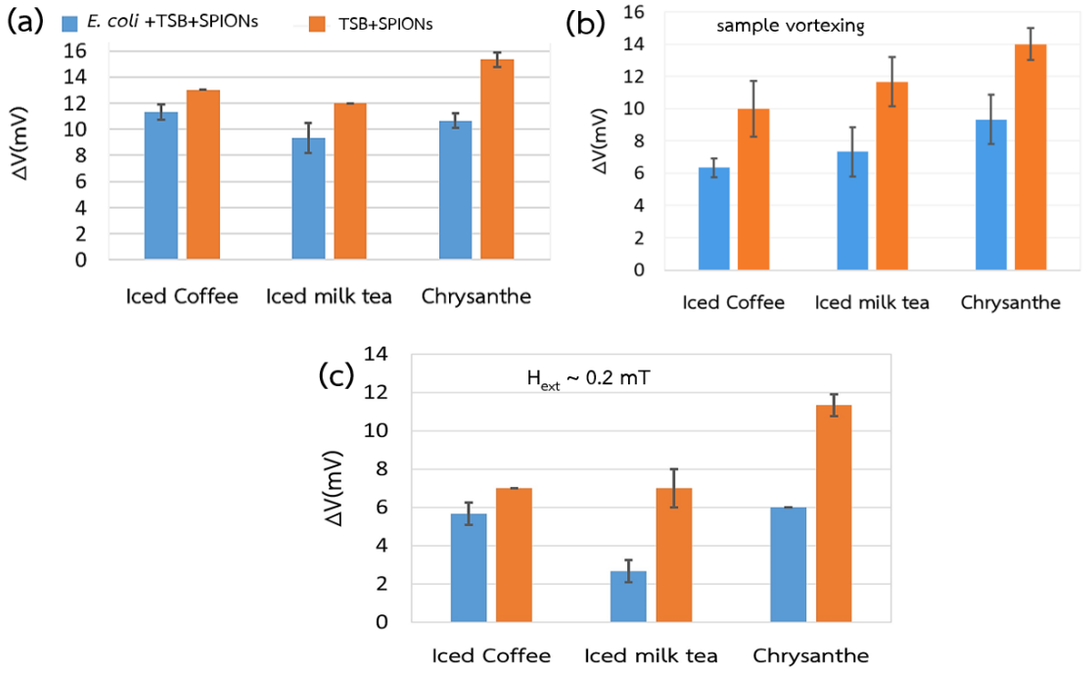

Figure 7. The output voltages (a) obtained from the MI-sensor from the iced coffee (S1), iced milk tea (S2), and chrysanthemum tea (S3) and their controls (C1-C3) after aggregating the samples for 10 min, (b) after applying a vortex mixture machine to suspend the mixtures, and (c) when changing the arrangement of the applied magnetic field H_{ext} ~0.2 mT in downward direction.

4. Conclusion

In summary, we have demonstrated the sensitivity of MI-sensor in detecting weak magnetic fields of few nanotesla without magnetic shielding. In particular, we employed the MI-sensor to detect the stray magnetic fields of SPIONs captured by *E. coli* bacteria with the concentration of 1.5 x 10^8 CFU/mL. Homogenization of the samples by vortexing the mixtures for 10 s prior to the detection and the application of the external static magnetic field (H_{ext}) ~ 0.2 mT toward the samples dramatically showed enhancement of the magnetic signals. In addition, common beverages, namely iced coffee, iced milk tea, and chrysanthemum tea were tested using the MI-sensor. Significant decreases in the corresponding output signals were observed, i.e., 1.67, 2.67, and 4.67 mV, for the iced coffee, iced milk tea, and chrysanthemum tea, respectively. Preliminary results indicated that the decrease of the magnetic moments is the result of the SPION captured by *E. coli* bacteria. These experimental results would lead to the determination of bacteria concentration and can be developed for magnetic biosensors.

Acknowledgment

This work was supported by Ubon Ratchathani University Research Fund.

References

Anik, M. I., Hossain, M. K., Hossain, I., Mahfuz, A. M. U. B., Rahman, M. T. and Ahmed, I. (2021). Recent progress of magnetic nanoparticles in biomedical applications: A review. **Nano Select**, 2(6), 1146-1186. doi:10.1002/nano.202000162

Bonilla, M., Kolekar, S., Ma, Y., Diaz, H. C., Kalappattil, V., Das, R., Eggers, T., Gutierrez R.G., Phan, M.-H. and Batzill, M. (2018). Strong room-temperature ferromagnetism in VSe2 monolayers on van der Waals substrates. **Nature Nanotechnology**, 13(4), 289-293. doi:10.1038/s41565-018-0063-9

Devkota, J., Ruiz, A., Mukherjee, P., Srikanth, H. and Phan, M.-H. (2013a). Magneto-Impedance Biosensor With Enhanced Sensitivity for Highly Sensitive Detection of Nanomag-D Beads. **IEEE Transactions on Magnetics**, 49(7), 4060-4063. doi:10.1109/tmag.2012.2235414

Devkota, J., Wang, C., Ruiz, A., Mohapatra, S., Mukherjee, P., Srikanth, H. and Phan, M. H. (2013b). Detection of low-concentration superparamagnetic nanoparticles using an integrated radio frequency magnetic biosensor. **Journal of Applied Physics**, 113(10), 104701. doi:10.1063/1.4795134

Krishnan, K. M. (2017). **Fundamentals and Applications of Magnetic Materials**. New York: Oxford University Press.

Li, Z., Ma, J., Ruan, J. and Zhuang, X. (2019). Using Positively Charged Magnetic Nanoparticles to Capture Bacteria at Ultralow Concentration. **Nanoscale Research Letters**, 14(1), 195. doi:10.1186/s11671-019-3005-z

Liu, J., Su, D., Wu, K. and Wang, J.-P. (2020). High-moment magnetic nanoparticles. **Journal of Nanoparticle Research**, 22(3). doi:10.1007/s11051-020-4758-0

Makarov, D., Melzer, M., Karnaushenko, D. and Schmidt, O. G. (2016). Shapeable magnetoelectronics. **Applied Physics Reviews**, 3(1), 011101. doi:10.1063/1.4938497

Moghanizadeh, A., Ashrafizadeh, F., Varshosaz, J. and Ferreira, A. (2021). Study the effect of static magnetic field intensity on drug delivery by magnetic nanoparticles. **Scientific Reports**, 11(1), 18056. doi:10.1038/s41598-021-97499-7

Mohri, K., Humphrey, F. B., Panina, L. V., Honkura, Y., Yamasaki, J., Uchiyama, T. and Hirami, M. (2009). Advances of amorphous wire magnetics over 27 years. **physica status solidi (a)**, 206(4), 601-607. doi:10.1002/pssa.200881252

Nakayama, S. and Uchiyama, T. (2015). Real-time measurement of biomagnetic vector fields in functional syncytium using amorphous metal. **Scientific Reports**, 5, 8837. doi:10.1038/srep08837

Quintana-Sánchez, S., Barrios-Gumiel, A., Sánchez-Nieves, J., Copa-Patiño, J. L., de la Mata, F. J. and Gómez, R. (2021). Bacteria capture with magnetic nanoparticles modified with cationic carbosilane dendritic systems. **Materials Science and Engineering: C**, 112622. doi:10.1016/j.msec.2021.112622

Sandhu A. and Handa H. (Ed.) (2018). **Magnetic Nanoparticles for Medical Diagnostics.** Bristal: IOP Publishing.

Sroysee, W., Ponlakhet, K., Chairam, S., Jarujamrus, P. and Amatatongchai, M. (2016). A sensitive and selective on-line amperometric sulfite biosensor using sulfite oxidase immobilized on a magnetite-gold-folate nanocomposite modified carbon-paste electrode. **Talanta**, 156-157, 154-162. doi:10.1016/j.talanta.2016.04.066

Steel, A. (March, 14, 2022). Ultra-sensitive magnetic sensor. Retrieved from https://www.aichi-steel.co.jp/ENGLISH/smart/mi/products/type-dh.html

Uchiyama, T., Nakayama, S., Mohri, K. and Bushida, K. (2009). Biomagnetic field detection using very high sensitivity magnetoimpedance sensors for medical applications. **physica status solidi (a)**, 206(4), 639-643. doi:10.1002/pssa.200881251

Wang, T., Zhou, Y., Lei, C., Luo, J., Xie, S. and Pu, H. (2017). Magnetic impedance biosensor: A review. **Biosensors and Bioelectronics**, 90, 418-435. doi:10.1016/j.bios.2016.10.031

Wu, W., Wu, Z., Yu, T., Jiang, C. and Kim, W. S. (2015). Recent progress on magnetic iron oxide nanoparticles: synthesis, surface functional strategies and biomedical applications. **Science and Technology of Advanced Materials**, 16(2), 023501. doi:10.1088/1468-6996/16/2/023501

Yang, Z., Liu, Y., Lei, C., Sun, X.-c. and Zhou, Y. (2015). A flexible giant magnetoimpedance-based biosensor for the determination of the biomarker C-reactive protein. **Microchimica Acta**, 182(15-16), 2411-2417. doi:10.1007/s00604-015-1587-4

Yang, Z., Liu, Y., Lei, C., Sun, X.-c. and Zhou, Y. (2016). Ultrasensitive detection and quantification of E. coli O157:H7 using a giant magnetoimpedance sensor in an open-surface microfluidic cavity covered with an antibody-modified gold surface. **Microchimica Acta**, 183(6), 1831-1837. doi:10.1007/s00604-016-1818-3

Zhong, J., Rosch, E. L., Viereck, T., Schilling, M. and Ludwig, F. (2021). Toward Rapid and Sensitive Detection of SARS-CoV-2 with Functionalized Magnetic Nanoparticles. **ACS Sensor**, 6(3), 976-984. doi:10.1021/acssensors.0c02160